Journal of Hydroscience and Hydraulic Engineering
Vol. 19, No.1 May, 2001, 85-96

DISCHARGE COEFFICIENT OF OBLIQUE SIDE-WEIRS

By

Masaru Ura, Yoshinori Kita, Juichiro Akiyama, Hirotaka Moriyama and Akhilesh Kumar Jha

Department of Civil Engineering, Kyushu Institute of Technology, Tobata, Kitakyushu, Japan

SYNOPSIS

An investigation of side-weirs, used as a diversion structure in rivers and channels, is presented. Most commonly, the side-weirs are aligned parallel to the direction of flow in the parent channel, giving a take-off angle of 90 degrees. However, these normal side-weirs have inherent disadvantage of reducing discharge coefficient at high Froude numbers in the parent flow. This study investigates performance of oblique side-weirs, that take-off at an angle less than 90 degrees. Discharge coefficients for oblique side-weirs are obtained theoretically and experimentally as function of take-off angle, Froude number in the parent channel and the weir geometry. It is found that a high value of discharge coefficient can be maintained when take-off angle lies between 60 and 80 degrees. An oblique side-weir with take-off angle equal to 70 degrees is selected for further studies with improved frontal apron and approach wall. It is concluded that the value of discharge coefficient can be further increased for a wide range of high Froude numbers through these improvements.

INTRODUCTION

Rivers and drainage channels running through urban areas frequently receive larger peak discharges than what they have been designed for. This phenomenon is caused by an increase in the runoff coefficient due to the development of road pavement and an unexpected expansion of urban areas in the river basin during the last few decades. Furthermore, in the last few years rainfalls with increased intensity in space and time are frequently observed in many areas. One of the many countermeasures for flood control is construction of side-weirs and flood retention ponds beside the river, when it is difficult to enlarge flow cross-sectional area in the lower reaches of the river because of urbanization along the river. The discharge in excess of the carrying capacity of the lower reaches is made to overflow the side-weir into the flood retention pond for temporary storage during the peak flood stages. The stored water is gradually released to the river after peak of the flood has passed.

Side-weirs are commonly aligned parallel to the direction of flow in rivers, giving take-off angle of 90 degrees. One of the principal equation for designing side-weirs is known as the De Marchi equation (1). For the discharge coefficient in the De Marchi equation, Subramanya and Awasthy (2) derived the functional relationship for the river

Froude number at the beginning of the weir region from theoretical considerations and systematic experiments. From their results it is clear that the discharge coefficient decreases from 0.6 to 0.45 when the Froude number increases from 0.1 to 0.6. This reduction in discharge coefficient with increasing Froude number in the parent channel makes side-weirs disadvantageous for flood control, because the peak stage of river flow will increase Froude number in the channel. It thus becomes necessary to construct a long weir for cutting off the excess discharge from the river and to ensure the safety of areas downstream. Ura et al. (3) modified the De Marchi equation and investigated the characteristics of discharge coefficient of the side-weir constructed in a trapezoidal channel having side slope 1V:mH. For a special case of side slope m=0, that is rectangular channel, the governing equations obtained by Ura et al.(3) coincided with that of De Marchi (1), and the experimental results of Ura et al.(3) coincided with that of Subramanya and Awasthy (2). Subramanya and Awasthy (2) suggested that the reduction in discharge coefficient due to increase in Froude number of the parent flow was caused by a reduction in the effective weir length normal to the overflow velocity vector.

This paper proposes oblique side-weirs that take-off at angles less than 90 degrees in order to increase the overflow angle against the side-weir. The characteristics of discharge coefficient of oblique side-weirs is investigated theoretically and experimentally as functions of take-off angle, Froude number in the parent channel and ratio of flow depth to the weir height. Improvement of shapes near the oblique side-weir is also investigated and suitable arrangements are proposed to obtain higher efficiency and practical performance. One of the improved type of oblique side-weirs is an oblique side-weir with front apron (named Type-F), and another one is an oblique side-weir with gradually expanding approach wall (named Type-G).

THEORETICAL CONSIDERATION

Side-weirs can be classified as normal or oblique depending on whet her they take off at 90 degrees or less than that. This study considers oblique side-weirs, constructed at one bank of the parent channel, having a rectangular cross section with channel width B ; and bottom slope i_0 ; as shown in Fig.1. The length of side-weir region L ; height of side-weir W ; take-off angle of oblique side-weir θ ; and other relevant parameters are shown in Figs.1 to 3.

Taking x-axis along flow direction of the parent channel (see Fig.1), y= water depth; A= cross sectional area; R= hydraulic radius; and Q= flow discharges at positions along the parent channel, the discharge q per unit length over the side-weir region L can be written by a continuity equation as

$$q = -dQ/dx \tag{1}$$

Specific energy E along the channel bottom is

$$E = y + \frac{Q^2}{2gB^2y^2} \tag{2}$$

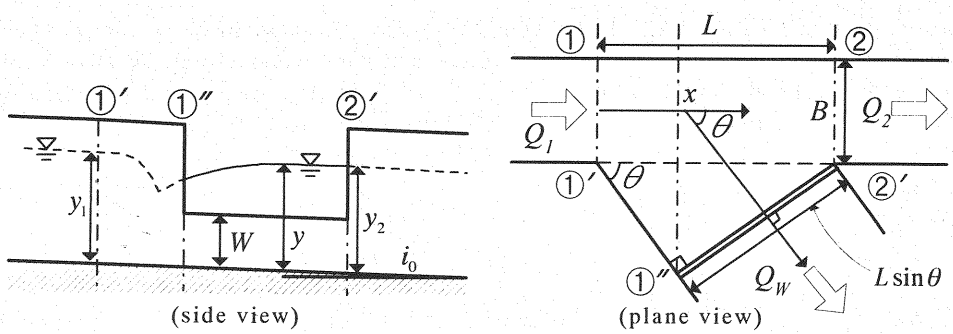

(side view) (plane view)

Fig.1 Oblique side-weir with take-off angle θ, Type-A

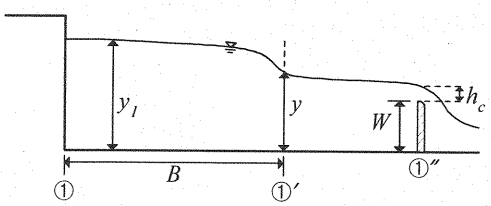

Fig.2 Vertical section of ①－①'－①''in Fig.1

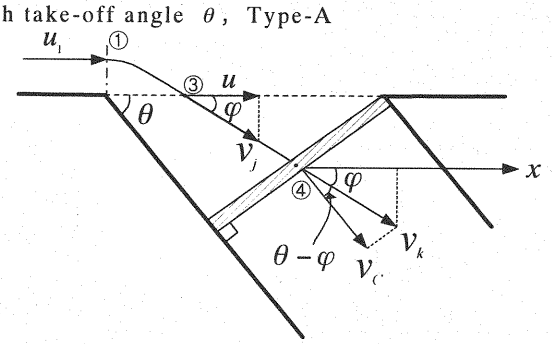

Fig.3 Flow direction and velocity near the

When the momentum principle is applied to the control volume ①-①'-①''-②'-② in Fig.1, the following differential equation for water depth accompanied by side flow is obtained

$$\frac{dy}{dx}=\frac{i_0-\dfrac{Q^2}{C_h{}^2RA^2}+\dfrac{\beta Qq}{gA^2}}{1-\dfrac{\beta Q^2B}{gA^3}} \tag{3}$$

where C_h= Chézys'resistance factor; β = momentum coefficient and g= gravitational acceleration. When the slope i_0 of the channel is not so steep, the first and the second terms in the numerator of Eq.3 are numerically almost equal. And assuming β is equal to unity in the case of a rectangular channel, Eq.3 can be simplified as follows

$$\frac{dy}{dx}=\frac{Qqy}{gB^2y^3-Q^2} \tag{4}$$

Next, the discharge q per unit length over the side-weir region is considered. Assuming that the velocity v_j at point ③ in Fig.3 has an angle φ with the parent flow, the following relationship is obtained.

$$\cos\varphi=u/v_j \tag{5}$$

where u=velocity of parent flow. The flow divided from the parent flow at the point ③ is supposed to maintain the flowing angle φ and to overflow with velocity v_k at the weir crest, point ④. The magnitude of overflow velocity v_k is assumed to be determined by a part of the specific energy in the parent flow at point ③. Thus,

$$y+\frac{\alpha_0 u^2}{2g}=h_c+W+\frac{v_k{}^2}{2g} \tag{6}$$

where α_0 is a factor accounting for contribution from the parent flow velocity head, and h_c is the flow depth over the weir. In the weir section the flow becomes critical. Thus the condition,

$$v_k{}^2/gh_c=1.0 \tag{7}$$

can be substituted into Eq.6, whereby

$$h_c=\frac{2}{3}\left(y-W+\frac{\alpha_0 u^2}{2g}\right) \tag{8}$$

$$v_k{}^2=\frac{2}{3}g\left(y-W+\frac{\alpha_0 u^2}{2g}\right) \tag{9}$$

are obtained. The overflow velocity component v_c perpendicular to the weir is expressed as

$$v_c=v_k\cos(\theta-\varphi) \tag{10}$$

Then the discharge q per unit length over the side-weir region is expressed as follows, with a local discharge coefficient C,

$$qdx=Cv_c h_c dx\sin\theta \tag{11}$$

Inserting Eqs.8, 9 and 10 into Eq.11, the following equation is obtained,

$$q=Cv_k h_c\cos(\theta-\varphi)\sin\theta$$

$$=\frac{2}{3}\sqrt{2g}(y-W)^{\frac{3}{2}}\frac{C}{\sqrt{3}}\left[1+\frac{\alpha_0 u^2}{2g(y-W)}\right]^{\frac{3}{2}}\cos(\theta-\varphi)\sin\theta \tag{12}$$

If we formally define an overall discharge coefficient C_M as

$$C_M = \frac{C}{\sqrt{3}}\left[1+\frac{\alpha_0 u^2}{2g(y-W)}\right]^{\frac{3}{2}}\cos(\theta-\varphi)\sin\theta \tag{13}$$

Eq.12 can be expressed as

$$q = \frac{2}{3}\sqrt{2g}(y-W)^{\frac{3}{2}}C_M \tag{14}$$

If Eqs.2 and 14 are inserted into Eq.4, then

$$\frac{dy}{dx} = \frac{4}{3}\frac{C_M}{B}\frac{\sqrt{(E-y)(y-W)^3}}{3y-2E} \tag{15}$$

is obtained. If C_M is assumed to be a constant with respect to x, Eq.15 can be integrated along x between section ① and ②(Fig.1), and the following equations are obtained,

$$x_2 - x_1 = L = \frac{3}{2}\frac{B}{C_M}(\phi_2 - \phi_1) \tag{16}$$

$$\phi_i(y_i, E_i) = \frac{2E_i - 3W}{E_i - W}\sqrt{\frac{E_i - y_i}{y_i - W}} - 3\tan^{-1}\sqrt{\frac{E_i - y_i}{y_i - W}} \tag{17}$$

where i=1 and 2 correspond to the cross-section at the upper and the lower end of the side-weir region, respectively. Eqs.16 and 17 are known as De Marchi equations.

The discharge coefficient C_M for the oblique side-weir with take-off angle θ, considered in this study, is governed by Eq.13. Numerical constants will be examined experimentally in the next section. Here, we introduce non-dimensional parameters normalized at the upper end of the side-weir region in the parent flow. The terms in the square bracket in Eq.13 can be expressed as

$$\left[1+\frac{\alpha_0 u^2}{2g(y-W)}\right] = \left[1+\frac{\alpha\gamma^2 F_1^2}{2(1-\eta)}\right] \tag{18}$$

$$F_1^2 = u_1^2/gy_1 = Q_1^2/gB^2y_1^3 \tag{19}$$

where F_1= Froude number at the upper end of the side-weir region in the parent flow

$$\eta = W/y_1 \tag{20}$$

$$\gamma = u/u_1 \tag{21}$$

$$\alpha = \alpha_0\cdot(1-\eta)/(y/y_1-\eta) \tag{22}$$

where α = modified contribution factor of parent velocity head, and y_1, u_1 and Q_1= water depth, mean velocity and flow discharge at the upper end of the side-weir region in the parent flow, respectively.

The angle φ in Eq.13 is formally defined by Eq.5. The magnitude of the angle φ as a function of F_1 is evaluated by assuming that the specific energy on a stream line at the point ① in Fig.3 is equal to that at the point ③, just before the flow diverges from the parent flow. Thus,

$$y_1 + \frac{u_1^2}{2g} = y + \frac{v_j^2}{2g} \tag{23}$$

The flow diverges from the parent flow at the point ③, where it is supposed to be a control section conforming to

$$v_j^2 / gy = 1.0 \tag{24}$$

Inserting Eq.24 into Eq.23, we get

$$v_j^2 = \frac{2}{3} g \left(y_1 + \frac{u_1^2}{2g} \right) \tag{25}$$

Furthermore, inserting Eq.25 into Eq.5, we get

$$\cos\varphi = \frac{u}{v_j} = \left(\frac{u^2}{v_j^2} \right)^{\frac{1}{2}} = \sqrt{\frac{u^2}{\frac{2}{3} g \left(y_1 + \frac{u_1^2}{2g} \right)}} = \sqrt{\frac{3\gamma^2 F_1^2}{2 + F_1^2}} \tag{26}$$

Finally, the discharge coefficient C_M is obtained from Eq.13, using Eqs.18 and 26 and, using C=1.06 as obtained from the experiments,

$$C_M = 0.611 \left[1 + \frac{\alpha\gamma^2 F_1^2}{2(1-\eta)} \right]^{\frac{3}{2}} \left(\cos\theta \sqrt{\frac{3\gamma^2 F_1^2}{2 + F_1^2}} + \sin\theta \sqrt{1 - \frac{3\gamma^2 F_1^2}{2 + F_1^2}} \right) \sin\theta \tag{27}$$

The factor α in Eq.27 expresses an effect of approach velocity on C_M, when α given by Eq.22 is used in place of α_0 in Eq.6. When this effect of approach velocity is negligible, depending on weir geometry or shape, Eq.27 is simplified by putting α = 0 as given below,

$$C_M = 0.611 \left(\cos\theta \sqrt{\frac{3\gamma^2 F_1^2}{2 + F_1^2}} + \sin\theta \sqrt{1 - \frac{3\gamma^2 F_1^2}{2 + F_1^2}} \right) \sin\theta \tag{28}$$

Further, in case of normal side-weirs, that is, when the take-off angle θ is equal to 90 degrees, $\cos\theta = 0$ and $\sin\theta = 1$. Thus, Eq.28 simplifies to,

$$C_M = 0.611\cos(\theta - \varphi)\sin\theta = 0.611\sqrt{1 - \frac{3\gamma^2 F_1^2}{2 + F_1^2}} \qquad (29)$$

If the coefficient γ is unity, Eq.29 becomes identical to the equation derived by Subramanya and Awasthy (2).

EXPERIMENTAL STUDY

Experimental study on oblique side-weirs was carried out in a rectangular channel 600cm long, 25cm high, 11.5cm wide and sloping 1 in 833. A side-weir region having length L =15cm is considered between section ① and ② as shown in Fig.1. The position x of section ① is at 350cm from the channel entrance. An oblique side-weir is set at the right side of the channel between section ① and ②. The take-off angle θ of the oblique side-weir is set to 40, 50, 60, 70, 80 and 90 degrees. The side-weir is sharp crested, 3cm high and $Lsin\theta$ long. Six sets of experiment were carried out by varying the take-off angle θ. For every θ, the water depth y_1 at section ① along the centerline of the parent channel was selected to be 5.0, 7.0 and 9.0cm, and Froude number at the upper side section ①, defined by Eq.19, was obtained as 0.4, 0.5, 0.6, 0.7 and 0.8. Measurements of water depths y_1 and y_2 at the channel section ①-①' and ②-②' were carried out by an ultrasonic displacement meter. Flow discharge Q_1 before the section ①-①' was obtained from the flow depth h_E over the sharp-crested weir set at the entrance of the parent channel as the measuring device. The relationship between h_E and Q_1 was calibrated before the experiments. Flow discharge Q_2 after the section ②-②'was obtained at the rectangular tank set below the parent channel end. The height h_0 in the tank was recorded with time t using wave height gauge. Thereafter Q_2 was evaluated as $(\Delta h_0/\Delta t)St$, where Δh_0 = incremental depth in the tank in time interval Δt and S_T = the surface area of the tank. Discharge over the side-weir Q_W was then calculated as $Q_W = Q_1 - Q_2$.

Experiments were carried out on three shapes of oblique side-weirs. These were;

Type-A: Simple oblique side-weirs that have the take-off angle less than 90 degrees as shown in Fig.1.

Type-F: Oblique side-weirs that have a frontal apron as shown in Fig.6.

Type-G: Oblique side-weirs that have a gradually expanding curved approach wall in addition to the Type-F side-weir as shown in Fig.7.

EXPERIMENTAL RESULTS

Experimental results for side-weirs with take-off angle θ=90 degrees and 70 degrees in Type-A, θ =70 degrees in Type-F and θ =70 degrees in Type-G are shown in Table.1. First, using the results of Type-A weirs, the relationships between discharge coefficient and Froude number of the parent channel at the upper end of side-weir region are shown in Fig.4 , each figure showing the relationship for the same take-off angle θ. In Fig.4, W/y_1 is used as a parameter and shown by symbols. The broad solid line is by Eq.27 using α=0 and γ =1.0 for every angle, fine line is by Eq.29 with γ =1.0, which coincides with the equation proposed by Subramanya and Awasthy(2) for normal side-weirs. Eq.29 with γ =1.0 for θ=90 degrees is plotted in every figure in Fig.4 for

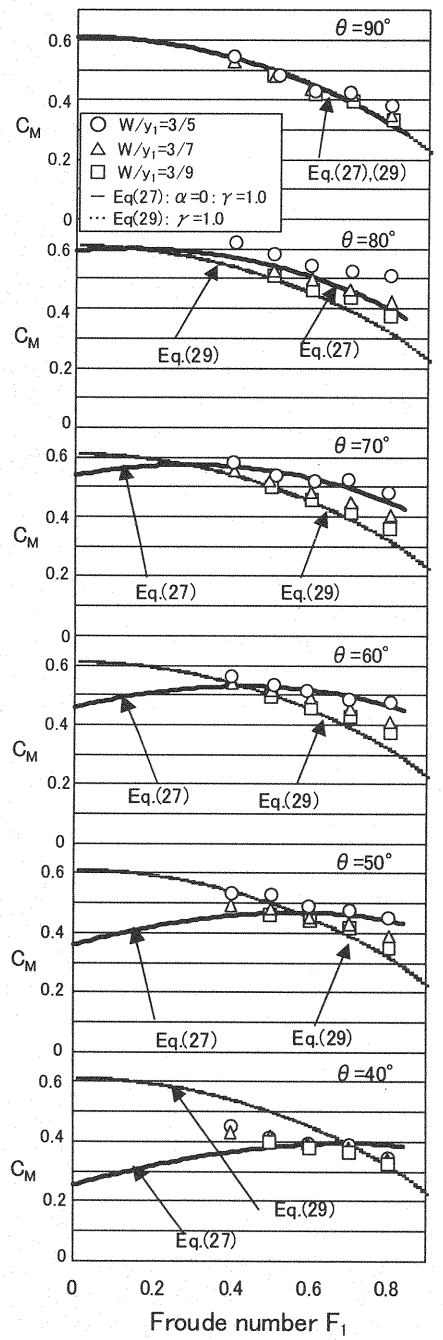

Fig.4 Relationships between discharge coefficient C_M and Froude number F_1 of Type-A

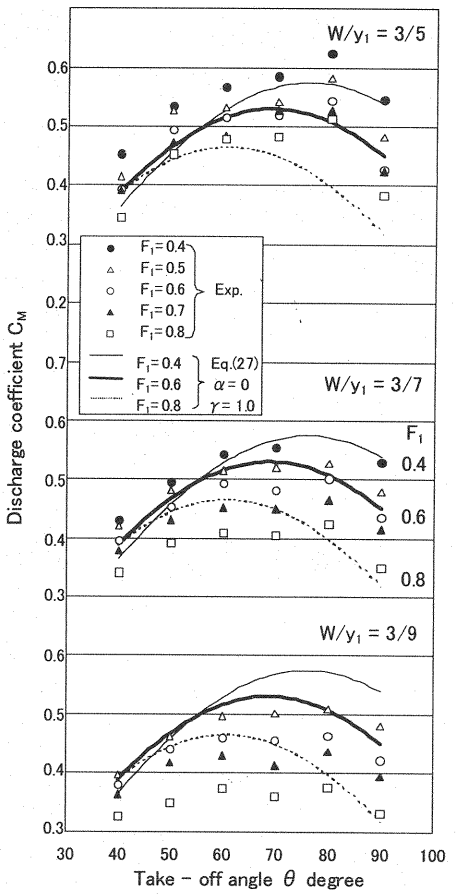

Fig.5 Relationships between C_M and θ of Type-A

easy comparison. From Fig.4, discharge coefficient of the oblique side-weirs is considered to be approximately expressed by Eq.27, with $\alpha=0$ and $\gamma=1.0$. There appears some difference depending on value of W/y_1 shown by symbols in Fig.4. It may be noted that when θ is between 60 and 80 degrees C_M becomes a little larger than when θ is 90 degrees, as long as F_1 remains between 0.4 and 0.9.

Next, we investigated the relationship between the discharge coefficient C_M and the take-off angle θ of oblique side-weirs, in Fig.5. The plots are under the condition of same W/y_1, using one symbol for one Froude number F_1. Three lines of fine, solid and dotted

in Fig.5 denote Eq.27 (α =0, γ = 1.0) for the Froude number value of 0.4, 0.6 and 0.8, respectively. The agreement of experimental values to the theoretical ones is not so good, but the theoretical lines qualitatively demonstrate that the maximum value of C_M can be achieved at an angle smaller than 90 degree, the angle becoming smaller with increasing Froude number F_1. From Figs.4 and 5, it is concluded that an oblique side-weir with take-off angle between 60 and 80 degrees can achieve a higher value of discharge coefficient C_M than a normal side-weir, if it is designed to draw from the parent channel having flow Froude number F_1 larger than 0.4.

INPROVEMENT OF OBLIQUE SIDE-WEIR

From the investigations in the preceding section, it is found that C_M can be improved even for higher parent channel Froude number, if the oblique side-weir takes off at an angle between 60 and 80 degrees. However, this will cause practical problems in case of Type-A oblique side-weirs. For example, flow separation might occur at the upper end of side-weir region ①'(Fig.1) because of sudden expansion in the channel width. Separation region would increase with increase in channel Froude number, decreasing the discharge coefficient C_M. In addition, at low Froude numbers and at water depth y_1 lower than W, the region ①'-①''-②'in front of the weir shown in Fig.1 will become dead water region, where suspended sediment or floating matters will get accumulated. To prevent forming of dead water regions in front of a side-weir, we propose to set a slope from the crest line ①''-②'of weir to the bottom line ①'-②'of the channel as shown in Fig.6. The oblique side-weir with this slope is named as the oblique side-weir with front apron or Type-F. In addition, to reduce the possibility of flow separation, a circular approach wall is added to the Type-F. This Type of oblique side-weir is named the oblique side-weir with gradually expanding front apron or Type-G as shown in Fig.7.

Experimental results on Type-F and Type-G with take-off angle of 70 degrees are also shown in Table.1. Relationships between C_M and F_1 on Type-A, Type-F and Type-G are shown in Fig.8, wherein the take-off angle is 70 degrees. Three solid

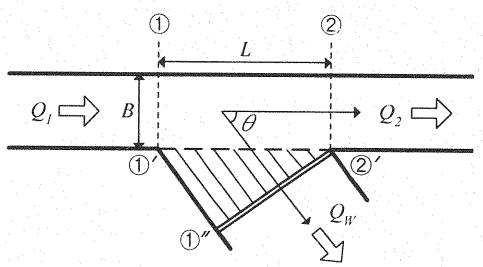

Fig.6(a) The oblique side-weir with front apron, Type-F (plane view)

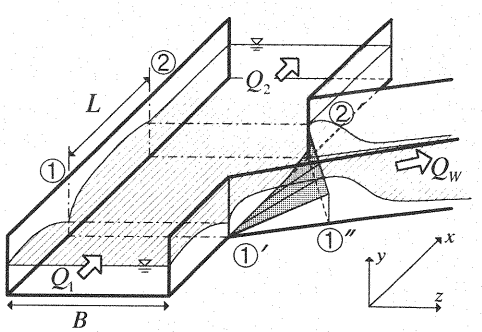

Fig.6(b) Type-F (perspective view)

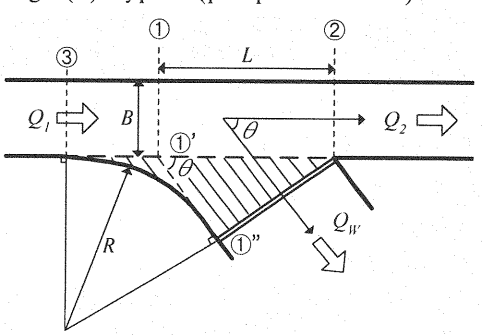

Fig.7 The oblique side-weir with gradually expanding approach wall and frontapron, Type-G (plane view)

lines in the figure use different values of α and γ in Eq.27 in order to fit with the experimental values. The dotted fine line is by the equation proposed by Subramanya and Awasthy(2) or Eq.29 with γ =1.0. From Fig.8 it is concluded that

1) the characteristics of discharge coefficient C_M of side-weir can be expressed generally by the Eq.27 with appropriate values of α and γ,
2) all types of oblique side-weir with take-off angle between 60 to 80 degrees have better discharge coefficients than normal side-weirs,
3) oblique side-weir of Type-F has larger C_M than that of Type-A, and
4) in the oblique side-weir of Type-G, the discharge coefficient is larger than 0.55 even when the parent channel Froude number is equal to 0.8.

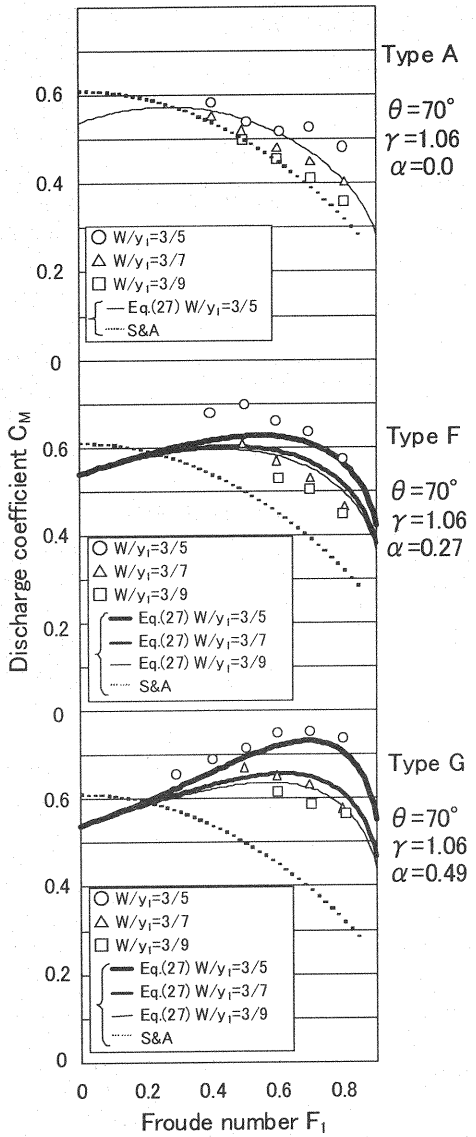

Fig.8 Relationships between C_M and F_1 of side-weirs in Type-A, Type-F and Type-G with take-off angle θ =70 degrees

CONCLUSIONS

In order to reduce flow discharge or water level at maximum or peak flow stages in rivers running through developed urban areas, side-weirs have been frequently used to divert excess discharge from the rivers to a retention pond for temporary storage. Side-weirs are advantageous as they don't obstacle the river flow and are free from maintenance. However, they have inherent disadvantage of reducing discharge coefficient with increasing river Froude number. Side-weirs designed for flood control must work efficiently at higher Froude numbers during peak flows. We have investigated theoretically and experimentally the oblique side-weirs, that take-off at angles less than 90 degrees, to minimize these inherent disadvantages. Oblique side-weirs with take-off angle θ between 60 to 80 degrees are found to give better performance. In order to improve practical problems of dead water region and flow separation, this study proposes oblique side-weirs with front apron or Type-F and that with gradually expanding approach wall or Type-G. The characteristics of discharge coefficient of oblique side-weir in Type-A, Type-F and Type-G can be expressed generally by Eq.27. The additional parameters α and γ in Eq.27 have been quantified experimentally in this study. Type-F weir with front apron has higher

discharge coefficient than Type-A oblique side-weir. Furthermore, Type-G, oblique side-weir with gradually expanding approach wall and front apron, has the highest discharge coefficient, larger than 0.55 even at the parent channel Froude number equal to 0.8. It is hoped that this study will contribute to the design of an efficient diversion structure for flood control.

Table.1 Experimental results
B=11.5cm, i_0=1/833, L=15.0cm, W=3.0cm

θ(°)	y_1 (cm)	y_2 (cm)	Q_1 (cc)	Q_2 (cc)	Q_W (cc)	F_1	C_M	θ(°)	y_1 (cm)	y_2 (cm)	Q_1 (cc)	Q_2 (cc)	Q_W (cc)	F_1	C_M
90 TypeA	5.01	5.24	1600	792	808	0.397	0.545	70 TypeA	4.99	5.21	1612	734	878	0.402	0.585
	5.00	5.26	2060	1216	844	0.512	0.483		4.98	5.25	2034	1099	934	0.508	0.542
	5.01	5.37	2437	1605	832	0.604	0.428		4.98	5.36	2433	1418	1015	0.608	0.518
	5.02	5.50	2823	1976	847	0.698	0.425		5.01	5.60	2811	1688	1123	0.697	0.528
	4.99	5.74	3219	2348	871	0.802	0.383		5.00	5.79	3214	2029	1186	0.799	0.483
	7.02	7.32	2658	499	2159	0.397	0.528		7.01	7.28	2687	418	2269	0.403	0.554
	7.02	7.46	3355	1210	2144	0.502	0.480		7.00	7.40	3292	986.5	2306	0.493	0.521
	7.03	7.61	3991	1847	2144	0.595	0.435		6.98	7.59	3989	1647	2342	0.601	0.481
	7.00	7.81	4666	2384	2282	0.701	0.416		6.99	7.84	4686	2217	2469	0.704	0.450
	6.99	7.99	5325	3100	2224	0.801	0.350		6.99	8.10	5353	2813	2540	0.804	0.405
	9.01	9.49	4860	1040	3820	0.499	0.481		9.01	9.46	4834	871	3962	0.497	0.501
	9.00	9.74	5877	2181	3696	0.604	0.422		9.00	9.58	5828	1811	4017	0.600	0.456
	9.00	10.01	6827	2990	3837	0.702	0.395		8.98	9.83	6820	2721	4098	0.703	0.413
	8.99	10.23	7809	4082	3727	0.805	0.331		9.01	10.16	7801	3778	4023	0.802	0.359
70 TypeF	4.99	5.24	1582	575	1007	0.395	0.681	70 Type G	4.99	5.33	1616	615	1001	0.403	0.692
	5.00	5.38	2008	852	1155	0.498	0.699		4.99	5.46	2021	888	1133	0.503	0.717
	5.00	5.45	2392	1141	1251	0.594	0.661		5.01	5.64	2409	1082	1326	0.597	0.750
	5.01	5.63	2797	1423	1373	0.693	0.636		5.00	5.79	2820	1264	1556	0.700	0.753
	5.00	5.81	3208	1751	1457	0.796	0.573		5.00	5.96	3208	1400	1808	0.796	0.739
	7.00	7.48	3299	637	2662	0.495	0.610		7.00	7.52	3325	395	2930	0.499	0.671
	6.99	7.61	3990	1213	2776	0.599	0.571		7.00	7.70	3993	856	3138	0.598	0.653
	6.99	7.81	4664	1753	2911	0.701	0.530		7.00	7.94	4655	1272	3383	0.698	0.632
	7.00	8.15	5353	2457	2896	0.804	0.465		6.99	8.07	5299	1747	3551	0.797	0.578
	9.00	9.68	5840	1268	4572	0.601	0.530		9.01	9.85	5841	618	5223	0.600	0.615
	9.00	10.02	6792	1979	4814	0.700	0.506		8.99	10.11	6807	1309	5499	0.702	0.588
	9.01	10.29	7776	2873	4903	0.799	0.449		8.99	10.46	7815	1844	5970	0.805	0.566

Acknowledgement:

The authors thank Mr. Hiroki Ono, former student of the Kyushu Institute of Technology for his vigorous assistance.

REFERENCES

1. De Marchi, G. :Suggio di teoria del funzionamento degli stramazzi laterali, L' Energia Elettrica, Milano, Italy, 11, pp.849-860, 1934.
2. Subramanya, K. and Awasthy, S.C. : Spatially varied flow over side-weir, Journal of the Hydraulics Division, ASCE, Vol.98, No.1, pp.1-10, 1972.
3. Ura,M., H.Ono, J.Akiyama and S.Sakamoto: Discharge formula and coefficient of side-weirs in a trapezoidal main channel (in Japanese), Annual Journal of Hydraulic Engineering, JSCE, vol.42, pp.691-696, 1998.

APPENDIX－NOTION

The following symbols are used in this paper ;

A	= cross sectional area ;
B	= width of parent channel ;
C, C_M	= discharge coefficient of side-weir ;
C_h	= Chézys′ resistance factor of parent channel ;
E, E_i	= specific energy ;
F_1	= Froude number at the cross-section of upper end of side-weir region in parent channel ;
g	= gravitational acceleration ;
h_c	= water depth over weir crest ;
i_0	= bottom slope of parent channel ;
L	= length of side-weir region along parent channel ;
q	= discharge per unit length over side-weir region ;
Q, Q_i	= discharge through a section ;
$Q_W=Q_1-Q_2$	= discharge over side-weir ;
R	= hydraulic radius in parent channel ;
u,u_i	= velocity at a section in parent flow ;
v_c	= normal velocity component over side-weir crest ;
v_j	= approach velocity toward side-weir ;
v_k	= velocity over side-weir crest ;
W	= height of side-weir ;
x, x_i	= distance along flow direction from the entrance of parent channel ;
y, y_i	= water depth at a section in parent flow ;
α, α_0	= contribution factor of parent flow velocity head on specific energy ;
β	= momentum coefficient ;
$\gamma=u/u_1$	= relative channel velocity in side-weir region ;
$\eta=W/y_1$	= ratio of weir height to water depth ;
θ	= take-off angle of oblique side-weir ;
ϕ_i	= De Marchi's varied flow function ;
φ	= approaching flow angle with parent flow direction ;

Suffix.

$i=1$	= cross section at the upper end of weir region in parent channel ; and
$i=2$	= cross section at the lower end of weir region in parent channel.

(Received August 14, 2000 ; revised December 22, 2000)